FULL PAPER *Biochemistry*

AP-1-Mediated Expression of Brain-Specific Class IVa β-Tubulin in P19 Embryonal Carcinoma Cells

Yuka MARUYAMA[1)], Kazuhiko ARAHARA[1)], Emi KINOSHITA[1)] and Katsuhiko ARAI[1)]*

[1)]*Department of Tissue Physiology, Tokyo University of Agriculture and Technology, Fuchu, Tokyo 183-8509, Japan*

(Received 2 July 2014/Accepted 25 August 2014/Published online in J-STAGE 26 September 2014)

ABSTRACT. Expression of brain-specific phenotypes increased in all *trans* retinoic acid (ATRA)-induced neural differentiation of mouse P19 embryonal carcinoma cells. Among these phenotypes, expression of class IVa β-tubulin isotype (TUBB4a) was particularly enhanced in neural differentiation. Transient transfection assays employing a reporter construct found that ATRA-mediated regulatory region of the TUBB4a gene lay in the region from −83 nt to +137 nt relative to the +1 transcription start site. Site-directed mutagenesis in the AP-1 binding site at −29/−17 suggested that the AP-1 binding site was a critical region for ATRA-mediated TUBB4a expression. Chromatin immunoprecipitation experiments suggested participation of JunD and activating transcription factor-2 (ATF2) in TUBB4a expression. Additionally, exogenous induction of the dominant-negative (dn) type of JunD canceled ATRA-induced upregulation of TUBB4a, and the dn type of ATF2 suppressed even the basal activity. Further immunoblot study revealed an ATRA-mediated increase in JunD protein, while a significant amount of ATF2 protein was constantly produced. These results suggest that differentiation-mediated activation of JunD results in enhanced TUBB4a expression.

KEY WORDS: embryonal carcinoma cell, neuronal differentiation, promoter analysis, retinoic acid, tubulin isotype

doi: 10.1292/jvms.14-0343; *J. Vet. Med. Sci.* 76(12): 1609–1615, 2014

Microtubules are composed of a heterodimer of α- and β-subunits and are dynamic structures that are constantly growing and shortening. Among these subunits, β-tubulins are classified into classes I, II, III, IVa, IVb, V and VI and highly conserved across vertebrate species with an isotype-specific variable region at the carboxyl terminus [3, 4, 21, 35]. Differential expression of β-tubulin isotypes has been observed during cellular differentiation in relation to organogenesis [15, 16, 35] or tumorigenesis [8, 21] and with the emergence of sublines that are resistant to anti-microtubule agents [5, 13, 18, 26, 30]. Some isotypes of β-tubulin manifest a characteristic cell-type distribution. In normal tissues of the nervous system, the class II isotype (TUBB2) is the major one [3, 4, 21], while class III (TUBB3) is known to be the neuron-specific isotype and is often used as a marker for neuronal differentiation [13]. In contrast, class IVa β-tubulin (TUBB4a) has been reported to be restricted to central nerve tissue [3, 21].

The mouse embryonal carcinoma cell line, P19, is derived from an embryo-derived teratocarcinoma and can differentiate into all three germ layers cell types [23]. P19 cells can differentiate into extraembryonic endoderm-like cells without the use of inducing factors [19] and into muscle-like cells in the presence of 1% DMSO [10, 14]. It is known that a low concentration (10 nM) of all *trans* retinoic acid (ATRA) can induce aggregated P19 cells to differentiate into primitive endoderm-like cells [22], whereas, at higher concentrations (0.5–1 μM), they differentiate into neurons and glial cells [1, 27, 29, 33]. Following ATRA-stimulated neural differentiation, it was found that P19 cells induced expression of TUBB3 [9, 11, 13] and neurofilament-M (NF-M) [32, 33].

It has been described that the effects of ATRA are mediated by ligand-dependent activation of RA receptors (RAR) that act directly as transcription factors modulating gene expression by interacting with RA response elements (RARE) in the regulatory region [34]. On the other hand, ATRA induced stimulation of ERK1/2 followed by rapid and sustained phosphorylation of the cyclic AMP response element binding protein (CREB) on neurite extension in rat neuronal cells [7]. Additionally, ATRA induced caspase-3-dependent apoptosis in Sertoli cells by activation of the MEK-ERK cascade [36]. These studies pointed out the RAR/RXR-independent mechanism in ATRA-mediated differentiation and apoptosis.

During examination of mechanism of ATRA-mediated upregulation of TUBB4a, we found that an AP-1 binding site in the promoter region was the critical element for *mTUBB4a* gene expression in neuronal differentiation in P19 cells. Consequently, we suggested that activation AP-1 upregulated the level of TUBB4a.

MATERIALS AND METHODS

Cell culture and neuronal differentiation: The P19 embryonal carcinoma cell line was purchased from the American Type Culture Collection (ATCC, Manassas, VA, U.S.A.), and the cells were cultured in α-MEM (Invitrogen Corp., Carlsbad, CA, U.S.A.) supplemented with 10% fetal calf serum (FBS, Sigma-Aldrich Chemical Co., St. Louis,

*CORRESPONDENCE TO: ARAI, K., Department of Tissue Physiology, Faculty of Agriculture, Tokyo University of Agriculture and Technology, Saiwai-cho 3–5–8, Fuchu, Tokyo 183-8509, Japan. e-mail: karai@cc.tuat.ac.jp

©2014 The Japanese Society of Veterinary Science

This is an open-access article distributed under the terms of the Creative Commons Attribution Non-Commercial No Derivatives (by-nc-nd) License <http://creativecommons.org/licenses/by-nc-nd/3.0/>.

Table 1. Primer sets for quantitative RT-PCR

Gene	Upper	Lower	Annealing temp	Size
NF-L	5′-GAAGAAGAAGGTGGTGAG-3′	5′-GAATAGTTGGGAATAGGG-3′	49.2°C	127 bp
NF-M	5′-TAATGGCTTAGATGTGAG-3′	5′-TGATGTATTTGGTAGCAC-3′	48.3°C	128 bp
MAP2	5′-GGAAGATGTAGGAGTGTC-3′	5′-ACTGTCTCTGTTTGATGC-3′	47.0°C	137 bp
TUBB2	5′-AACCTTTGTGTCCTAACG-3′	5′-CTTCTCATTGTTGGATTG-3′	47.0°C	208 bp
TUBB3	5′-GAGGAGGAGGGGGAGATG-3′	5′-GGCTAAAATGGGGAGGAC-3′	56.3°C	271 bp
TUBB4a	5′-CTCTCACCTTGCCTTACC-3′	5′-ATTTATTGATGGAGGGTC-3′	53.1°C	229 bp
GAPDH	5′-CTCCCACTCTTCCACCTTCG-3′	5′-CCACCACCCTGTTGCTGTAG-3′	53.4°C	110 bp

Table 2. Primer sets for amplification of regulatory regions in the *mTUBB4a* gene

Construct name		Sequence	Site	Annealing temp	Size	Cloning site
mTUBB4aL	Upper	5′-GGCACGCGTGCAAGGAACACAGCAAGTAGCAC-3′	–1145 / −1123	63.1°C	1649 bp	*Mlu*I
	Lower	5′-GGCAAGCTTTGTTAGTCGGGAAGGGCTGAGAG-3′	+484 / +504			*Hind*III
mTUBB4aM	Upper	5′-GGCACGGCTCAGAGTGGAAAGAAAGAATGGTG-3′	–360 / −338	63.5°C	894 bp	*Mlu*I
	Lower	5′-GGCAAGCTTGTGCTAAGATGTCAGAGTGGGTC-3′	+511 / +534			*Hind*III
mTUBB4aS	Upper	5′-GGCACGGCTCTCCGCAGCCATCTCGTC-3′	–83 / −66	63.6°C	220 bp	*Mlu*I
	Lower	5′-GGCAAGCTTTTCCTGGGTGAGCCTTGG-3′	+120 / +137			*Hind*III

The underline area in each sequence indicates an artificially-introduced cutting site of the restriction enzyme for subcloning into the pGL3 plasmid vector.

MO, U.S.A.) supplemented with a penicillin-streptomycin-neomycin mixture (Invitrogen) in an atmosphere of humidified air and 5% CO_2 at 37°C. Subconfluent P19 cells that had been propagated in a monolayer were used as the control (C). For neural differentiation, P19 cells were seeded in a bacterial grade petri dish with medium containing 0.5 μM ATRA and cultured for 4 days, and then cell aggregates were washed with PBS, trypsinized, plated onto a gelatin-coated culture dish and cultured in the absence of ATRA to promote neurodifferentiation (D; differentiated cells). Total cell RNA was extracted with TRIZOL (Invitrogen) according to the manufacturer's instructions. Complementary DNA was prepared by reverse transcription with Transcriptor Reverse Transcriptase (Roche Diagnostics, Mannheim, Germany) and used for quantitative RT-PCR (qRT-PCR) using SYBR Premix Ex Taq II (Takara Bio Inc., Otsu, Japan). Primer sets for qRT-PCR are listed in Table 1. The levels of each mRNA were normalized against the GAPDH mRNA level. Three independent experiments from each cell culture sample were performed.

Construction of a reporter plasmid and site-directed mutagenesis: The promoter region of the mouse TUBB4a gene (*mTUBB4a*) was amplified by PCR using LATaq DNA Polymerase (Takara). Mouse genomic DNA was prepared from the C57BL/6 mouse liver and used as the template for PCR. The three primer sets listed in Table 2 were designed using the sequence derived from GenBank accession No. AK013717. These amplification products (1649 bp, 894 bp and 220 bp fragments, respectively) were digested with *Mlu*I and *Hind*III and subcloned into the pGL3 basic vector (Promega, Madison, WI, U.S.A.); the modified vectors were designated as p*mTUBB4aL-luc* (−1145/+504), p*mTUBB4aM-luc* (−360/+534) and p*mTUBB4aS-luc* (−83/+137), respectively (see Fig. 2A). A QuikChange XL Site-Directed Mutagenesis Kit (Stratagene, La Jolla, CA, U.S.A.) was used to introduce a point mutation into the potential AP-1 binding site at −29/−17 in p*mTUBB4aS-luc* (see Fig. 3A) and designated AP-1m. Briefly, the AP-1 sequence was changed from CATCAGACGCCAC to CATCAGACGCttt; the mutated site is indicated with lowercase letters. The mutation constructs were verified by DNA sequencing. Plasmids were purified using an EndoFree Plasmid Maxi kit (Qiagen, Inc., Valencia, CA, U.S.A.) according to the manufacturer's instructions and used for the transfection experiments described below.

Electrophoresis mobility shift assay (EMSA): A complementary single-strand oligonucleotide containing the putative AP-1 site (5′- CCGGTCGACACCCGTCCATCAGACGCCACCA-3′, −46/−14) was annealed and 3′ end-labeled with DIG-11-ddUTP (Roche Diagnostics) using terminal transferase (Roche Diagnostics). The mutated probe (5′-CCGGTCGACACCCGTCCATCAGACGCtttCA-3′; the mutated site is indicated with lowercase letters) was designated as AP-1m. Nuclear proteins were extracted with a CelLytic Nuclear Extraction Kit (Sigma-Aldrich) according to the manufacturer's instruction. An equal amount of nuclear protein was mixed with Gel Shift Binding Buffer (Promega) and DIG-endo-labeled duplex oligonucleotide and then incubated for 15 min at room temperature. For the competition assay, an excess amount of unlabeled probe corresponding to the AP-1 consensus sequence (5′- CGCTTGATGACTCAGCCGGAA-3′, Santa Cruz Biotechnology Inc., Santa Cruz, CA, U.S.A.) or the mutation-introduced probe (AP-1m) was incubated with nuclear extracts prior to being mixed with the labeled probe. DNA-protein complexes were separated on 5% non-denaturing polyacrylamide gels

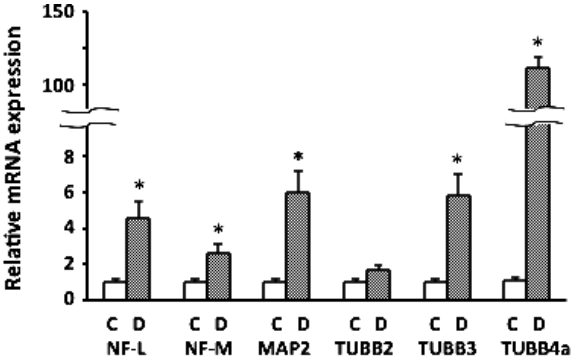

Fig. 1. Quantitative RT-PCR (qRT-PCR) analysis of the mRNA level corresponding to NF-L, NF-M. MAP2, TUBB2, TUBB3 and TUBB4a. P19 cells in the growth phase were treated with 0.5 μM ATRA for 4 days to form neurospheres, and then the neurospheres were dispersed and cultured on gelatin-coated dishes for 2 days to induce neural differentiation (D). Total RNA was extracted and analyzed by qRT-PCR. The values shown are means ± SD of three independent experiments. Asterisks indicate a significant difference (P<0.05) from undifferentiated control cells (C).

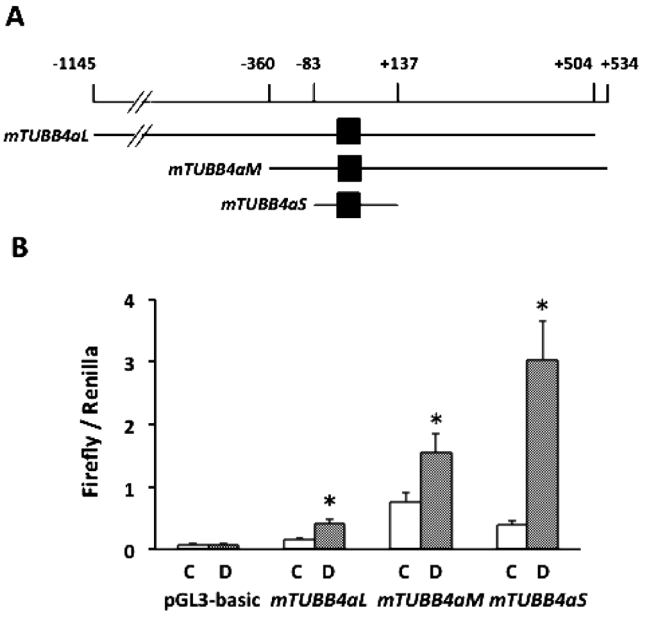

Fig. 2. Schematic representation of the promoter region of the *mTUBB4a* gene. Three different lengths of PCR products were amplified and subcloned into pGL3-basic vector. The closed box indicates the first exon. P19 cells were pretreated to form neurospheres as described above, and then the neurospheres were dispersed and cultured on gelatin-coated dishes. After overnight culture, control (C) and ATRA-treated P19 cells (D) were transfected with pGL3-basic vector subcloned with *mTUBB4aL* (−1145/+504), *mTUBB4aM* (−360/+534) and *mTUBB4aS* (−83/+137), respectively, and then cultured overnight. At the end of cultivation, the luciferase activity in the supernatant of cell lysate was analyzed. The values shown are means ± SD of three independent experiments. Asterisks indicate a significant difference (P<0.05) from undifferentiated control cells (C).

supplemented with 3.33% Rhinohide Polyacrylamide Gel Strengthener (Molecular Probes Inc., Eugene, OR, U.S.A.) in 0.25 × Tris borate/EDTA at 4°C and 50 V. Gels were transferred onto a positively charged nylon membrane. After the separated fragments were fixed by UV cross-linking, the positive signals were visualized using the CSPD (Roche Diagnostics)-mediated chemiluminescence method. Positive signals were obtained by exposure to X-ray film (Hyperfilm ECL, GE Healthcare, Buckinghamshire, U.K.).

Cell transfection and luciferase assay: Transient transfection of P19 cells was performed using the FuGENE HD transfection reagent (Roche Diagnostics). P19 cell aggregates, which had been treated with ATRA for 4 days, were trypsinized, and 5×10^4 cells were seeded onto gelatin-coated 12-well culture plates (3.8 cm^2/well). The same number of control P19 cells was seeded onto similar plates. Following overnight culture, the medium was replaced with 5% FBS/α-MEM, and then control and ATRA-treated P19 cells in each well were transfected with a mixture containing 6 μl of FuGENE HD and 1 μg of a construct in 100 μl of Opti-MEM I (Invitrogen). To assess transfection efficiency, 2.5 ng of p*RL-tk* vector (Promega), which encodes a Renilla luciferase gene downstream from a thymidine kinase (*tk*) enhancer and immediate-early promoter, was systemically added to the transfection mixture. In the case of forced expression experiments, 1 μg of dominant-negative-type c-Jun [2], JunD [24], c-Fos [28], CREB1 [28] or ATF2 [6] was added to the transfection mixture. The total amount of DNA for each transfection was kept constant using the empty vector pcDNA3.1 (Invitrogen). Five hours after transfection, cell layers were replaced with 10% FBS/α-MEM and cultured for additional 24 hr. At the end of culture, cell layers were harvested with 100 μl of Passive Lysis Buffer (Promega), and the luciferase activity was assayed with a dual-luciferase reporter assay system (Promega) using a microtiter plate luminometer (Luminescencer JNR, ATTO, Tokyo, Japan). The activities of firefly luciferase were normalized against *Renilla* luciferase activity.

Chromatin immunoprecipitation (ChIP): A ChIP assay was performed using a commercial kit (Upstate Biotechnology, Charlottesville, VA, U.S.A.) according to the manufacturer's instructions. Briefly, control and ATRA-treated cells were immediately fixed with 1% paraformaldehyde for 10 min at 37°C and sonicated. One percent of sheared DNA was saved as input DNA, and the other was immunoprecipitated with antibodies to c-Jun, JunD, c-Fos, CREB1, ATF-2 (all from Santa Cruz) or histone H3 (Cell Signaling Technology, Danvers, MA, U.S.A.). Precipitated DNA-protein complexes were digested with proteinase K and purified with a spin column. The resulting DNA fragments along with input DNA were used for quantitative PCR (qPCR) using an upper primer (at −80/−63; 5′-CGCAGCCATCTCGTCCAG-3′) and a lower primer (at +113/+130; 5′-GTGAGCCTTGGGAGAGCC-3′), which amplified a 210 bp fragment. The data are represented as the percentage vs. input DNA.

Immunoblot analysis: To compare the levels of JunD

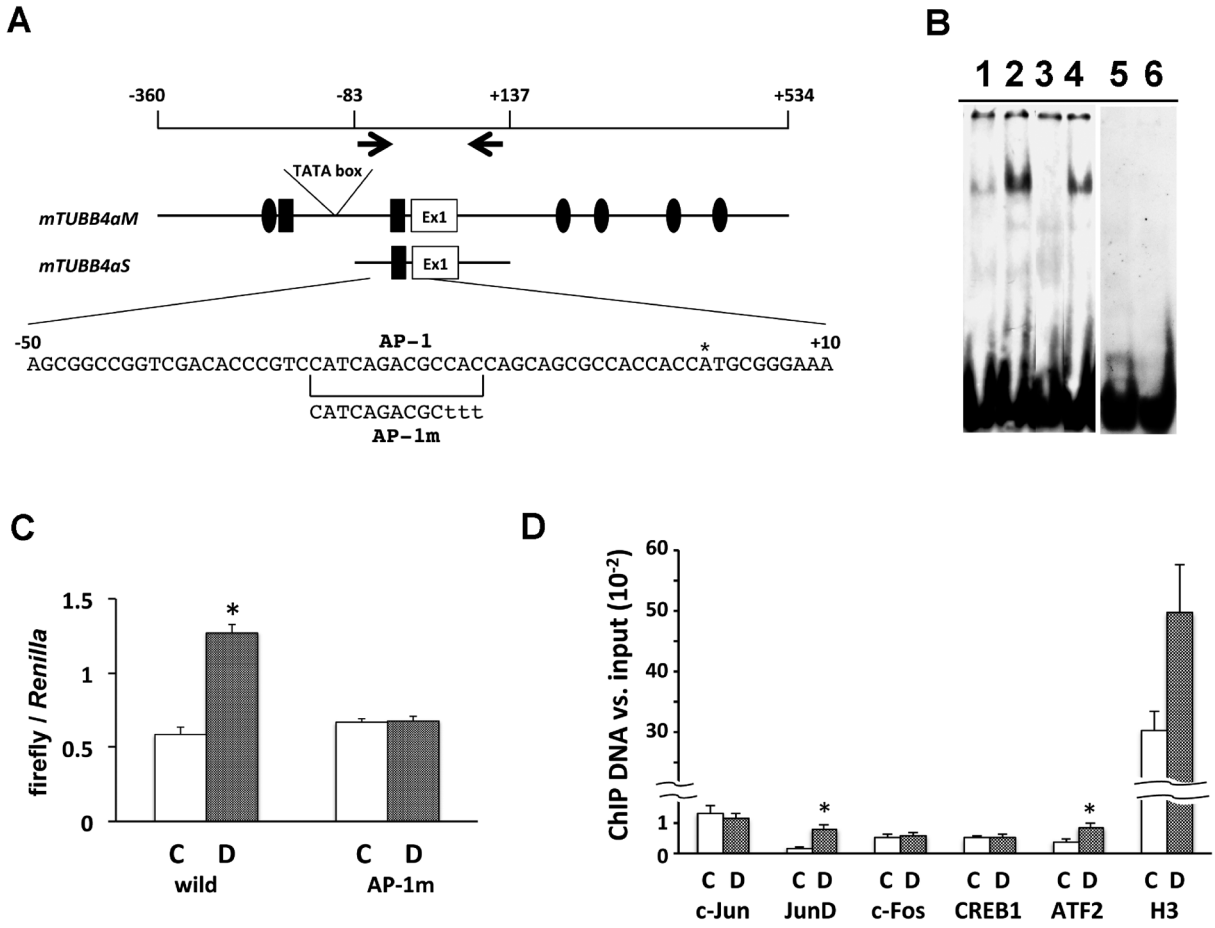

Fig. 3. A. Presumptive transcription factor binding sites of the promoter region and first intron of *mTUBB4aM* and *TUBB4aS*. A. The sequence contained within nucleotides −360 and + 534 nt of the *mTUBB4aM* gene was analyzed using a web-based search engine. Two putative AP-1 sites (closed box) and five Sp1 sites (closed oval) are indicated, and the first exon of the gene is boxed; an asterisk indicates a transcription start site. Two arrows indicate primer sites of the amplified region for the ChIP assay. The mutant in the AP-1binding site (−29/−17) within the promoter region of *mTUBB4aS* is indicated as AP-1m. The sequence of the AP-1 site is CATCAGACGCCAC, while that of AP-1m is CATCAGACGCttt; lowercase letters indicates the mutation site. B. EMSA was performed using DIG-labeled wild and AP-1-mutated probes. Nuclear protein extracted from undifferentiated P19 cells and cells undergoing neural differentiation: lanes 1 and 5, nuclear protein from control cells; lanes 2–4 and 6, nuclear protein from neurodifferentiated P19 cells. Competition experiments were performed with a 250-fold excess of an unlabeled consensus AP-1 probe (lane 3) and the mutated probe (lane 4). EMSA with a DIG-labeled mutated probe is shown in lanes 5 and 6. C. Control (C) and ATRA-treated P19 cells (D) were transfected with 1 μg of the p*mTUBB4aS-luc* or its mutants and 100 *n*g of p*RL-tk* for 5 hr. The medium was replaced, incubation was performed overnight, the cell layers were harvested, and then the luciferase activity was measured and normalized to *Renilla* luciferase activity. The values are means ± SD and are representative of three independent experiments. D. Control (C) and ATRA-treated P19 cells (D) were used for ChIP-qPCR. The antibodies to c-Jun, JunD, c-Fos, CREB1 and ATF2 used for immunoprecipitation are indicated. Anti-histone H3 antibody (H3) was used for the positive control. Data are shown as means ± SD of three independent experiments.

and ATF2 proteins in control and neurodifferentiated cells, immunoblot analysis of nuclear lysates was performed. Protein bands separated by SDS-PAGE were transferred onto a PVDF membrane and incubated with the appropriate antibody. After washing, the membrane was incubated with an HRP-labeled second antibody, and then the positive signals were detected on X-ray film with ECL Advance (GE Healthcare).

Statistical analysis: Statistical differences between the values of the respective experimental groups and controls were determined by Mann-Whitney's *U* test, and a value of $P<0.05$ was considered significant.

RESULTS

Enhanced TUBB4 expression in neural differentiation of P19 cells: All neural phenotypes examined in this study increased in ATRA-treated cells. Among these, NF-L, NF-M, microtubule associated protein-2 (MAP2) and class II and class III β-tubulin were upregulated 2- to 5-fold compared

with the control. On the other hand, expression of TUBB4a was extremely increased in differentiating cells, and the mRNA level was 100-fold greater than that in control cells (Fig. 1).

Characterization of the differentiation responsive region in the mTUBB4a gene: To investigate the regulation of *mTUBB4a* gene transcription during neural differentiation of P19 cells, three different lengths of PCR fragments were amplified and subcloned into pGL3 basic vector, and then a luciferase assay was performed. As a result, all luciferase constructs showed increased activities in neurodifferentiated P19 cells, and the shortest construct, p*mTUBB4aS-luc*, had the highest activity among the three constructs (Fig. 2). These results suggested that suppressor *cis*-elements lay in the upstream or downstream region of *mTUBB4aS*. Putative transcription factor binding sites were identified using the web-based search engine TRANSFAC (http://www.biobase-international.com/product/transcription-factor-binding-sites) to examine the PCR product; this analysis found two potential AP-1 sites (at −150/−139 and −29/−17) and one Sp1 site (at −167/−154) in the promoter region, and four Sp1 sites (at +154/+163, +200/+212, +291/303 and +358/+368) were identified in the first intron of *mTUBB4aM*, while *mTUBB4aS* contained only one AP-1 site (at −29/−17, Fig. 3A). Mutations were introduced into the AP-1 site found in *mTUBB4aS* (AP-1m), with the mutated sites being confirmed by competitive EMSA. The DNA-protein complex was very weak in the control cells and elevated in ATRA-induced P19 cells. Competition with the consensus AP-1 probe completely neutralized the positive signal, while the mutated probe lost the competition activity (Fig. 3B). Mutation of an AP-1 site prevented ATRA-mediated upregulation of the luciferase activity of *mTUBB4a*S (Fig. 3C), suggesting the participation of AP-1 family transcription factors in the expression of mTUBB4a. To identify AP-1 family member participating ATRA-mediated stimulation of mTUBB4a expression, ChIP followed by qPCR (ChIP-qPCR) was performed. ChIP-qPCR revealed that ATRA treatment promoted a 5-fold increase in JunD and that binding of ATF2 also increase slightly, whereas c-Jun, c-Fos and CREB1 were unaffected (Fig. 3D). Histone H3 was used as a positive control for the ChIP assay. The results indicated binding of JunD and ATF2 in the AP-1 site.

Effect of forced expression of transcription factors in the AP-1 family on the luciferase activity of TUBB4 gene: The ChIP assay indicated that JunD and ATF2 bound to the regulatory region of the *mTUBB4a* gene. To further confirm this, forced expression of AP-1 family genes in P19 cells was performed. As a result, co-transfection of dominant-negative JunD or ATF2 abrogated the effect of ATRA on the transcriptional activity of *mTUBB4aS* (Fig. 4A), whereas the dominant-negative form of c-Jun, c-Fos and CREB1 did not affect ATRA-mediated upregulation of the promoter activity. Additionally, dominant-negative ATF2 suppressed the basal luciferase activity of *mTUBB4a*S. Further, immunoblot analysis confirmed an elevated amount of JunD protein in the nuclear extract from ATRA-treated neurodifferentiated cells (Fig. 4B); a considerable amount of ATF2 protein was synthesized in the ATRA-untreated cells, but it was not affected by ATRA treatment.

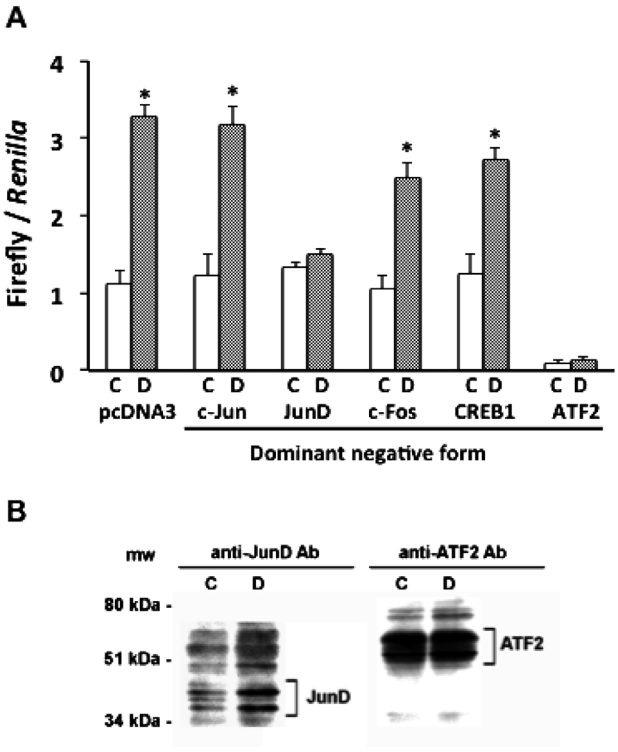

Fig. 4. A. Effect of the dominant-negative forms of c-Jun, JunD c-Fos, CREB1 or ATF2 on the stimulation of promoter activity for *mTUBB4aS* mediated by neuronal differentiation. Control (C) and ATRA-treated (D) P19 cells transfected with p*mTUBB4aS-luc*, p*RL-tk* and one of the expression vectors or the empty vector pcDNA3. Luciferase activity was measured and normalized against the *Renilla* luciferase activity. The values shown are mean ± SD of three representative and independent experiments. Asterisks indicate a significant difference ($P<0.05$) from undifferentiated cells. B. Western blot of cellular protein extracts from control (C) and differentiated (D) P19 cells using an antibody to JunD or ATF2. mw: molecular weight.

DISCUSSION

Expression of TUBB4a was previously shown to be highly restricted to central nerve tissue [3, 21], but the mechanism responsible for this transcriptional regulation remained unclear. In this study, we showed that TUBB4a was extremely increased in neurodifferentiated P19 cells compared with other well-known neuronal phenotypes including neurofilaments and TUBB3, and we identified a regulatory element of the *mTUBB4a* gene that was related to ATRA-mediated neural differentiation. To identify the regulatory region of *mTUBB4a*, we examined the region from −1145 nt to +534 nt in the *mTUBB4a* gene and suggested that the −83 upstream or +137 downstream region might contain a suppressor of the gene expression. Comparing three luciferase constructs, it was revealed that response elements for expression of

the gene during neural differentiation were present in the −83/+120 region and that there was an AP-1 binding site at −29/−17 in this region. Mutation of the AP-1 site (AP-1m) inhibited differentiation-mediated upregulation of the luciferase activity of *mTUBB4aS*, and further ChIP experiments showed binding of JunD and ATF2 to the region around the AP-1 binding site. These observations were confirmed by the results of exogenous overexpression of dominant-negative vectors, and differentiation-mediated upregulation of the luciferase activity was canceled by co-transfection of dominant-negative JunD or ATF2. Further, immunoblot analysis demonstrated an elevated level of JunD in differentiated P19 cells, suggesting that JunD could be a component of the AP-1 complex, while a high level of ATF2 proteins was observed even in undifferentiated P19 cells.

It was reported that ATF-2 plays a critical role in differentiation in P19 cells and overexpression of the dominant-negative form of ATF-2 reduced the promoter activities of several specific genes and inhibited differentiation of P19 [25]. Additionally, ATF-2 has been shown to be ubiquitously expressed in various human embryonic tissues and cell lines, with the highest expression level being observed in the brain [31]. Our present study showed the binding of ATF2 in the regulatory region of the *mTUBB4a* gene and showed that dominant-negative ATF2 suppressed the basal level in addition to the ATRA-mediated increase in expression. These results suggested that ATF2 played a significant role in regulation of the expression of the *mTUBB4a* gene in P19 cells. On the other hand, ATRA activates c-Jun amino-terminal kinase (JNK) through MAPK kinase 4 (MKK4) during induced neural differentiation in P19 cells [1]. ATRA also activates c-Jun, JunD and Fra-2 during the differentiation of P19 cells into cardiomyocytes [12]. In another embryonal carcinoma cell line, mouse F9, ATRA-dependent upregulation of c-Jun is mediated by an interaction of ATF-2 and p300 [20], and ATRA-induced differentiation results in a increase of c-Jun in the differentiation of F9 cells, suggesting that the activation of AP-1 by ATRA may play an important role in the events that result in differentiation [17]. Collectively, upregulation of *mTUBB4a* during ATRA-induced neural differentiation in P19 cells appears to be mediated by activation of the AP-1 complex. Further studies on signal transduction and the subsequent activation of JunD by ATRA together with the cooperation of JunD and ATF2 will be necessary to fully elucidate this process.

Taken together, our data presented here indicate that ATRA-induced neurodifferentiation of P19 cells could induce an enhanced TUBB4a mRNA level through activation of AP-1.

ACKNOWLEDGMENTS. This work was supported in part by a Grant-in-Aid from the Ministry of Education, Culture, Sports, Science and Technology of Japan (Grant No. 22580305). We are grateful to Dr. Jawed Alam (Alton Ochsner Medical Foundation, New Orleans, LA, U.S.A.), Prof. Derek A. Mann (Southampton General Hospital, Southampton, U.K.), Dr. V Rishi (NCI, NIH, Bethesda, MD, U.S.A.) and Prof. Ze'ev Ronai (Ruttenberg Cancer Center, Mount Sinai School of Medicine, New York, NY, U.S.A.) for kindly providing the dominant-negative vectors for c-Jun, JunD, c-Fos, CREB1 and ATF2, respectively.

REFERENCES

1. Akiyama, S., Yonezawa, T., Kudo, T. A., Li, M. G., Wang, H., Ito, M., Yoshioka, K., Ninomiya-Tsuji, J., Matsumoto, K., Kanamaru, R., Tamura, S. and Kobayashi, T. 2004. Activation mechanism of c-Jun amino-terminal kinase in the course of neural differentiation of P19 embryonic carcinoma cells. *J. Biol. Chem.* **279**: 36616–36620. [Medline] [CrossRef]
2. Alam, J., Stewart, D., Touchard, C., Boinapally, S., Choi, A. M. and Cook, J. L. 1999. Nrf2, a Cap'n'Collar transcription factor, regulates induction of the heme oxygenase-1 gene. *J. Biol. Chem.* **274**: 26071–26078. [Medline] [CrossRef]
3. Arai, K., Maruo, K., Ara, K. Y., Uehara, K. and Matsuda, H. 2001. Characterization of isotype-specific regions of five classes of canine beta-tubulin and their expression in several tissues and cell culture. *J. Vet. Med. Sci.* **63**: 1297–1302. [Medline] [CrossRef]
4. Arai, K., Shibutani, M. and Matsuda, H. 2002. Distribution of the class II beta-tubulin in developmental and adult rat tissues. *Cell Motil. Cytoskeleton* **52**: 174–182. [Medline] [CrossRef]
5. Arai, K., Matsumoto, Y., Nagashima, Y. and Yagasaki, K. 2006. Regulation of class II beta-tubulin expression by tumor suppressor p53 protein in mouse melanoma cells in response to Vinca alkaloid. *Mol. Cancer Res.* **4**: 247–255. [Medline] [CrossRef]
6. Bhoumik, A., Jones, N. and Ronai, Z. 2004. Transcriptional switch by activating transcription factor 2-derived peptide sensitizes melanoma cells to apoptosis and inhibits their tumorigenicity. *Proc. Natl. Acad. Sci. U.S.A.* **101**: 4222–4227. [Medline] [CrossRef]
7. Cañón, E., Cosgaya, J. M., Scsucova, S. and Aranda, A. 2004. Rapid effects of retinoic acid on CREB and ERK phosphorylation in neuronal cells. *Mol. Biol. Cell* **15**: 5583–5592. [Medline] [CrossRef]
8. Caracciolo, V., D'Agostino, L., Dráberová, E., Sládková, V., Crozier-Fitzgerald, C., Agamanolis, D. P., de Chadarévian, J. P., Legido, A., Giordano, A., Dráber, P. and Katsetos, C. D. 2010. Differential expression and cellular distribution of gamma-tubulin and betaIII-tubulin in medulloblastomas and human medulloblastoma cell lines. *J. Cell. Physiol.* **223**: 519–529. [Medline]
9. Dai, J. P., Lu, J. Y., Zhang, Y. and Shen, Y. F. 2010. Jmjd3 activates Mash1 gene in RA-induced neuronal differentiation of P19 cells. *J. Cell. Biochem.* **110**: 1457–1463. [Medline] [CrossRef]
10. Ding, B., Liu, C. J., Huang, Y., Yu, J., Kong, W. and Lengyel, P. 2006. p204 protein overcomes the inhibition of the differentiation of P19 murine embryonal carcinoma cells to beating cardiac myocytes by Id proteins. *J. Biol. Chem.* **281**: 14893–14906. [Medline] [CrossRef]
11. Endo, M., Antonyak, M. A. and Cerione, R. A. 2009. Cdc42-mTOR signaling pathway controls Hes5 and Pax6 expression in retinoic acid-dependent neural differentiation. *J. Biol. Chem.* **284**: 5107–5118. [Medline] [CrossRef]
12. Eriksson, M. and Leppä, S. 2002. Mitogen-activated protein kinases and activator protein 1 are required for proliferation and cardiomyocyte differentiation of P19 embryonal carcinoma cells. *J. Biol. Chem.* **277**: 15992–16001. [Medline] [CrossRef]
13. Gan, P. P. and Kavallaris, M. 2008. Tubulin-targeted drug action: functional significance of class ii and class IVb beta-tubulin in vinca alkaloid sensitivity. *Cancer Res.* **68**: 9817–9824. [Medline] [CrossRef]

14. Gianakopoulos, P. J., Mehta, V., Voronova, A., Cao, Y., Yao, Z., Coutu, J., Wang, X., Waddington, M. S., Tapscott, S. J. and Skerjanc, I. S. 2011. MyoD directly up-regulates premyogenic mesoderm factors during induction of skeletal myogenesis in stem cells. *J. Biol. Chem.* **286**: 2517–2525. [Medline] [CrossRef]
15. Hallworth, R. and Ludueña, R. F. 2000. Differential expression of beta tubulin isotypes in the adult gerbil cochlea. *Hear. Res.* **148**: 161–172. [Medline] [CrossRef]
16. Jensen-Smith, H. C., Eley, J., Steyger, P. S., Ludueña, R. F. and Hallworth, R. 2003. Cell type-specific reduction of beta tubulin isotypes synthesized in the developing gerbil organ of Corti. *J. Neurocytol.* **32**: 185–197. [Medline] [CrossRef]
17. Jin, C., Li, H., Murata, T., Sun, K., Horikoshi, M., Chiu, R. and Yokoyama, K. K. 2002. JDP2, a repressor of AP-1, recruits a histone deacetylase 3 complex to inhibit the retinoic acid-induced differentiation of F9 cells. *Mol. Cell. Biol.* **22**: 4815–4826. [Medline] [CrossRef]
18. Kamath, K., Wilson, L., Cabral, F. and Jordan, M. A. 2005. BetaIII-tubulin induces paclitaxel resistance in association with reduced effects on microtubule dynamic instability. *J. Biol. Chem.* **280**: 12902–12907. [Medline] [CrossRef]
19. Karperien, M., Farih-Sips, H., Hendriks, J. A., Lanske, B., Papapoulos, S. E., Abou-Samra, A. B., Löwik, C. W. and Defize, L. H. 1999. Identification of a retinoic acid-inducible element in the murine PTH/PTHrP (parathyroid hormone/parathyroid hormone-related peptide) receptor gene. *Mol. Endocrinol.* **13**: 1183–1196. [Medline] [CrossRef]
20. Kawasaki, H., Song, J., Eckner, R., Ugai, H., Chiu, R., Taira, K., Shi, Y., Jones, N. and Yokoyama, K. K. 1998. p300 and ATF-2 are components of the DRF complex, which regulates retinoic acid- and E1A-mediated transcription of the c-jun gene in F9 cells. *Genes Dev.* **12**: 233–245. [Medline] [CrossRef]
21. Leandro-García, L. J., Leskelä, S., Landa, I., Montero-Conde, C., López-Jiménez, E., Letón, R., Cascón, A., Robledo, M. and Rodríguez-Antona, C. 2010. Tumoral and tissue-specific expression of the major human beta-tubulin isotypes. *Cytoskeleton (Hoboken)* **67**: 214–223. [Medline] [CrossRef]
22. Lee, Y. N., Malbon, C. C. and Wang, H. Y. 2004. G alpha 13 signals via p115RhoGEF cascades regulating JNK1 and primitive endoderm formation. *J. Biol. Chem.* **279**: 54896–54904. [Medline] [CrossRef]
23. McBurney, M. W., Jones-Villeneuve, E. M., Edwards, M. K. and Anderson, P. J. 1982. Control of muscle and neuronal differentiation in a cultured embryonal carcinoma cell line. *Nature* **299**: 165–167. [Medline] [CrossRef]
24. Mann, J., Oakley, F., Johnson, P. W. and Mann, D. A. 2002. CD40 induces interleukin-6 gene transcription in dendritic cells: regulation by TRAF2, AP-1, NF-kappa B, AND CBF1. *J. Biol. Chem.* **277**: 17125–17138. [Medline] [CrossRef]
25. Monzen, K., Hiroi, Y., Kudoh, S., Akazawa, H., Oka, T., Takimoto, E., Hayashi, D., Hosoda, T., Kawabata, M., Miyazono, K., Ishii, S., Yazaki, Y., Nagai, R. and Komuro, I. 2001. Smads, TAK1, and their common target ATF-2 play a critical role in cardiomyocyte differentiation. *J. Cell Biol.* **153**: 687–698. [Medline] [CrossRef]
26. Nicoletti, M. I., Valoti, G., Giannakakou, P., Zhan, Z., Kim, J. H., Lucchini, V., Landoni, F., Mayo, J. G., Giavazzi, R. and Fojo, T. 2001. Expression of beta-tubulin isotypes in human ovarian carcinoma xenografts and in a sub-panel of human cancer cell lines from the NCI-Anticancer Drug Screen: correlation with sensitivity to microtubule active agents. *Clin. Cancer Res.* **7**: 2912–2922. [Medline]
27. Resende, R. R., Alves, A. S., Britto, L. R. and Ulrich, H. 2008. Role of acetylcholine receptors in proliferation and differentiation of P19 embryonal carcinoma cells. *Exp. Cell Res.* **314**: 1429–1443. [Medline] [CrossRef]
28. Rishi, V., Potter, T., Laudeman, J., Reinhart, R., Silvers, T., Selby, M., Stevenson, T., Krosky, P., Stephen, A. G., Acharya, A., Moll, J., Oh, W. J., Scudiero, D., Shoemaker, R. H. and Vinson, C. 2005. A high-throughput fluorescence-anisotropy screen that identifies small molecule inhibitors of the DNA binding of B-ZIP transcription factors. *Anal. Biochem.* **340**: 259–271. [Medline] [CrossRef]
29. Rujano, M. A., Pina, P., Servitja, J. M., Ahumada, A. M., Picatoste, F., Farrés, J. and Sabrià, J. 2004. Retinoic acid-induced differentiation into astrocytes and glutamatergic neurons is associated with expression of functional and activable phospholipase D. *Biochem. Biophys. Res. Commun.* **316**: 387–392. [Medline] [CrossRef]
30. Shalli, K., Brown, I., Heys, S. D. and Schofield, A. C. 2005. Alterations of β-tubulin isotypes in breast cancer cells resistant to docetaxel. *FASEB J.* **19**: 1299–1301. [Medline]
31. Takeda, J., Maekawa, T., Sudo, T., Seino, Y., Imura, H., Saito, N., Tanaka, C. and Ishii, S. 1991. Expression of the CRE-BP1 transcriptional regulator binding to the cyclic AMP response element in central nervous system, regenerating liver, and human tumors. *Oncogene* **6**: 1009–1014. [Medline]
32. Tang, K., Yang, J., Gao, X., Wang, C., Liu, L., Kitani, H., Atsumi, T. and Jing, N. 2002. Wnt-1 promotes neuronal differentiation and inhibits gliogenesis in P19 cells. *Biochem. Biophys. Res. Commun.* **293**: 167–173. [Medline] [CrossRef]
33. Wang, C., Xia, C., Bian, W., Liu, L., Lin, W., Chen, Y. G., Ang, S. L. and Jing, N. 2006. Cell aggregation-induced FGF8 elevation is essential for P19 cell neural differentiation. *Mol. Biol. Cell* **17**: 3075–3084. [Medline] [CrossRef]
34. Wei, L. N., Lee, C. H. and Chang, L. 1995. Retinoic acid induction of mouse cellular retinoic acid-binding protein-I gene expression is enhanced by sphinganine. *Mol. Cell. Endocrinol.* **111**: 207–211. [Medline] [CrossRef]
35. Yang, H., Ganguly, A., Yin, S. and Cabral, F. 2011. Megakaryocyte lineage-specific class VI β-tubulin suppresses microtubule dynamics, fragments microtubules, and blocks cell division. *Cytoskeleton (Hoboken)* **68**: 175–187. [Medline] [CrossRef]
36. Zanotto-Filho, A., Cammarota, M., Gelain, D. P., Oliveira, R. B., Delgado-Cañedo, A., Dalmolin, R. J., Pasquali, M. A. and Moreira, J. C. 2008. Retinoic acid induces apoptosis by a non-classical mechanism of ERK1/2 activation. *Toxicol. In Vitro* **22**: 1205–1212. [Medline] [CrossRef]